

ESTIMATION TECHNIQUE FOR CHARACTERIZING INHOMOGENEOUS CONDUCTING ZONE RELATED TO EDDY CURRENT TESTING

Adrian AUSRI and Fumio KOJIMA

- 1) Graduate School of Science and Technology, Kobe University (1-1,Rokkodai, Nada, Kobe 657-8501 JAPAN, E-mail: ausri@buna.fan.scitec.kobe-u.ac.jp)
- 2) Graduate School of Science and Technology, Kobe University (1-1,Rokkodai, Nada, Kobe 657-8501 JAPAN, E-mail: kojima@koala.kobe-u.ac.jp)

This paper describes an estimation technique for recovering internal profiles of stress corrosion cracking (SCC) related to eddy current testing in the sample material. First, mathematical description of eddy current model is formulated by a variational form defined in appropriate Hilbert spaces. Secondly, taking into account that SCC can be described by inhomogeneous conductivities in the sample material, the admissible parameter class is reconstructed by the set of electrical conductivities corresponding to the set of sub-regions in the suspect region. The method for recovering is directed to electromagnetic inverse problem by characterizing each sub-region of the SCC decomposition using its electrical conductivity, while an estimation technique for inverse analysis is proposed by a hybrid use of the forward analysis and inspection data. Finally, the feasibility and applicability of the proposed method are demonstrated through the computational experiments.

Key Words: Parameter Estimation, Identification, Inverse Problems, Nondestructive Evaluation, Electromagnetics

1. Introduction

Recently, due to the aged deterioration by small cracks and corrosion embedded in the material system of power plants, interest has grown for structural integrity of nuclear power plants. Inverse analysis on quantitative nondestructive evaluation is a key technology for safety and reassurance of the plants.

An electromagnetic nondestructive evaluation is to find a material flaw or a degradation level by evaluating structure-sensitive electromagnetic properties from measurement data related to eddy current testing (ECT). In this paper, we consider a domain identification problem associated with a stress corrosion cracking based on an eddy current model⁽²⁾⁽⁴⁾ to recover internal profiles of SCC arising in ECT. In Section 2, mathematical description of eddy current model is formulated by a variational form defined in appropriate Hilbert spaces related to a forward analysis. In Section 3, taking

into account that SCC can be described by inhomogeneous conductivities in the sample material, the admissible parameter class is reconstructed by the set of electrical conductivities corresponding to the set of sub-regions in the suspect region. Since the method for recovering is directed to electromagnetic inverse problem by characterizing each sub-region of the SCC decomposition using its electrical conductivity, then in Section 4, we discuss a estimation technique for inverse analysis to recover internal profiles of SCC, formulated by a hybrid use of the forward analysis and inspection data. Finally, the feasibility and applicability of the proposed method are demonstrated through the computational experiments.

2. Eddy current model

Let us assume that Ω be a bounded region in R^3 with a Lipschitz-continuous boundary Γ . We also suppose that a conducting and nonmagnetic material Ω_c is a sub-region of Ω . Then we set an air region as $\Omega_{air} = \Omega - \Omega_c$ (Fig.

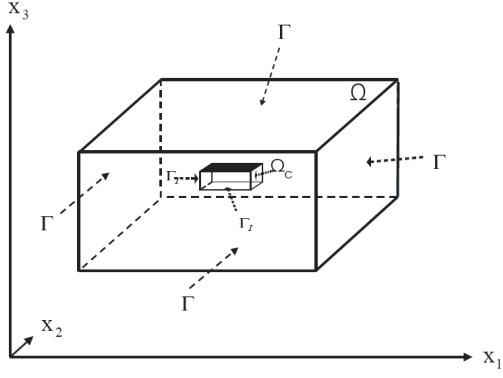


Fig. 1 Virtual box and sample material.

1) with the Lipschitz-continuous interface Γ_I . We introduce the magnetic vector potential $\mathbf{A} = (A_1, A_2, A_3)$ in Ω and the electrical scalar potential ϕ in Ω_c . By considering the Coulomb gauge condition ($\nabla \cdot \mathbf{A} = 0$), a three-dimensional eddy current problem in the conducting material Ω_c is governed by the equations:

$$-\frac{1}{\mu_0} \nabla^2 \mathbf{A} = -\sqrt{-1} \sigma_c \omega \mathbf{A} - \sigma_c \nabla \phi, \quad (1)$$

$$\nabla \cdot (\sqrt{-1} \sigma_c \omega \mathbf{A} + \sigma_c \nabla \phi) = 0, \quad \text{in } \Omega_c, \quad (2)$$

where ω , μ_0 , and σ_c denote an exciting angular frequency, a magnetic permeability of air, and an electrical conductivity of the sample material, respectively. The governing equation in the air region Ω_{air} is expressed by:

$$-\frac{1}{\mu_0} \nabla^2 \mathbf{A} = \chi_s \mathbf{J}_s, \quad (3)$$

with \mathbf{J}_s denotes the intensity of the exciting coil probe, while on the boundary Γ , we can impose the condition

$$\mathbf{A} = 0, \quad \text{on } \Gamma, \quad (4)$$

and on the interface Γ_I , we also impose the conditions

$$\mathbf{A}|_{\Omega_c} = \mathbf{A}|_{\Omega_{air}}, \quad \text{on } \Gamma_I, \quad (5)$$

$$\nabla \mathbf{A} \cdot \mathbf{n}|_{\Omega_c} = \nabla \mathbf{A} \cdot \mathbf{n}|_{\Omega_{air}}, \quad \text{on } \Gamma_I, \quad (6)$$

$$(\sqrt{-1} \sigma_c \omega \mathbf{A} + \sigma_c \nabla \phi) \cdot \mathbf{n}|_{\Omega_c} = 0, \quad \text{on } \Gamma_I. \quad (7)$$

Thus the eddy current density \mathbf{J}_e in the conducting material Ω_c can be evaluated by

$$\mathbf{J}_e = -\sqrt{-1} \sigma_c \omega \mathbf{A} - \sigma_c \nabla \phi. \quad (8)$$

Furthermore, we consider strategies for measurements of ECT signal made by means of transmitter-receiver coil pairs (See Kojima⁽²⁾⁽⁴⁾). Then, the observation by receiver coil can be represented by

$$\mathcal{Z}_{x_p}(\omega, \mathbf{J}_s) = -\sqrt{-1} N \omega \oint_{C(x_p)} \mathbf{A} \cdot d\mathbf{l}, \quad (9)$$

with N and $C(x_p)$ ($C \subset \Omega_{air}$) denote the number of coil turns and the center coordinate of the receiver coil, respectively.

In order to set up the computational schemes for the solution of the problems (1-7) using a finite element method which involves the integral equations, then in the sequel we introduce Hilbert spaces:

$$\begin{aligned} \mathcal{H} &:= ((L^2(\Omega))^3 \times L^2(\Omega_c)) \times ((L^2(\Omega))^3 \times L^2(\Omega_c)), \\ \mathcal{V} &:= ((H_0^1(\Omega))^3 \times H^1(\Omega_c)) \times ((H_0^1(\Omega))^3 \times H^1(\Omega_c)), \end{aligned}$$

where $H_0^1(\Omega) = \{\varphi \in H^1(\Omega) \mid \varphi = 0 \text{ on } \Gamma\}$.

We then define $\mathbf{u} := \{(\mathbf{A}^R, \phi^R), (\mathbf{A}^I, \phi^I)\} \in \mathcal{V}$, and $\mathbf{v} := \{(\mathbf{v}^R, \psi^R), (\mathbf{v}^I, \psi^I)\} \in \mathcal{V}$, with $\mathbf{v}^R = (v_1^R, v_2^R, v_3^R)$ and $\mathbf{v}^I = (v_1^I, v_2^I, v_3^I)$. Thus, for any $\mathbf{u}, \mathbf{v} \in \mathcal{V}$, the bilinear form on $\mathcal{V} \times \mathcal{V}$ can be defined as

$$\begin{aligned} \alpha_\omega(\mathbf{u}, \mathbf{v}) &:= \frac{1}{\mu_0} \sum_{i=1}^3 \int_{\Omega} (\nabla A_i^R \cdot \nabla v_i^R + \nabla A_i^I \cdot \nabla v_i^I) dx \\ &+ \int_{\Omega_c} (\nabla \phi^R \cdot \sigma_c \nabla \psi^R + \nabla \phi^I \cdot \sigma_c \nabla \psi^I) dx \\ &+ \omega \int_{\Omega_c} \sigma_c (\mathbf{A}^R \cdot \mathbf{v}^I - \mathbf{A}^I \cdot \mathbf{v}^R) dx \\ &+ \int_{\Omega_c} \sigma_c (\nabla \phi^R \cdot \mathbf{v}^R + \nabla \phi^I \cdot \mathbf{v}^I) dx \\ &+ \omega \int_{\Omega_c} \sigma_c (\mathbf{A}^R \cdot \nabla \psi^I - \mathbf{A}^I \cdot \nabla \psi^R) dx \quad (10) \end{aligned}$$

and the linear form on \mathcal{H} can be defined by

$$\beta_{\mathbf{J}_s}(\mathbf{v}) = \int_{C(x_p)} \chi_s \mathbf{J}_s \cdot \mathbf{v}^R dx. \quad (11)$$

Applying the set of alternating currents $\mathbf{J}_s \in (L^2(\Omega))^3$ and assuming that the angular frequency ω is properly chosen such that $0 < \omega \leq \omega_0 < \infty$ together with the set of electrical conductivities

$$\{\sigma_c \in W_\infty^0(\overline{\Omega_c}) \mid 0 < \bar{\sigma} \leq \sigma_c, \text{ in } \overline{\Omega_c}\},$$

we can find the set of a magnetic vector potential \mathbf{A} and an electrical scalar potential ϕ , which is a unique solution $\mathbf{u}(\omega, \mathbf{J}_s) = (\mathbf{A}, \phi) \in \mathcal{V}$ of the system (Eqs. (10) and (11))

$$\alpha_\omega(\mathbf{u}, \mathbf{v}) = \beta_{\mathbf{J}_s}(\mathbf{v}), \quad \text{for } \mathbf{v} \in \mathcal{H}. \quad (12)$$

Let us suppose that $l = \{1, 2, \dots, L\}$ be the index of coil positions. Relating to the above formulation, then the measurements model (9) can be reformulated as:

$$\begin{aligned} \mathcal{Z}^L(\omega, \mathbf{J}_s) &= \{\mathcal{Z}_{x_p^l}(\omega, \mathbf{J}_s)\}_{l=1}^L = \{N \omega \oint_{C(x_p^l)} \mathbf{A}^I \cdot d\mathbf{l}, \\ &- N \omega \oint_{C(x_p^l)} \mathbf{A}^R \cdot d\mathbf{l}\}_{l=1}^L, \quad (13) \end{aligned}$$

where $\mathbf{A}^R = (A_1^R, A_2^R, A_3^R)$ and $\mathbf{A}^I = (A_1^I, A_2^I, A_3^I)$ and with

$$A_j^R = \mu_0 \int_{\Omega_c} u^R J_{(s)j}^R dx, \quad A_j^I = \mu_0 \int_{\Omega_c} u^I J_{(s)j}^I dx, \quad (14)$$

$j = 1, 2, 3$ and where $C(x_p^l) \subset \Omega_{air}$ and $\mathbf{u} = (\mathbf{A}, \phi)$ with $\mathbf{A} = (\mathbf{A}^R, \mathbf{A}^I)$, denote the center coordinate of the receiver coil and the solution of the problem (12), respectively.

3. Admissible parameter class

Our problem here is to recover the internal profiles of SCC as shown in Fig. 2. The method for recovering is directed to electromagnetic inverse problem by characterizing each sub-region of the SCC decomposition using its electrical conductivity⁽⁵⁾. For this purpose, we suppose that a conducting material Ω_c is decompose into sub-regions Ω_{SCC} and $\Omega_c - \Omega_{SCC}$. And then a sub-region Ω_{SCC} is decomposed into M sub-regions Ω_{SCC}^k , $k = 1, 2, \dots, M$. We also assume that the electrical conductivity for each sub-region Ω_{SCC}^k is given by a constant σ_k . Therefore, the electrical conductivity σ_c for each sub-region Ω_{SCC}^k and a sub-region $\Omega_c - \Omega_{SCC}$ is then defined by

$$\sigma_c^k(\mathbf{x}) := \begin{cases} \sigma_0, & \text{for } \mathbf{x} \in \Omega_c - \Omega_{SCC}, \\ \sigma_k, & \text{for } \mathbf{x} \in \Omega_{SCC}^k, \quad k = 1, 2, \dots, M, \end{cases}$$

where $\{\sigma_k\}_{k=1}^M$ belong to the admissible parameter class

$$\mathcal{Q}^M = \{ \{ \sigma_k \}_{k=1}^M \mid 0 < \bar{\sigma} \leq \sigma_k \leq \sigma_0 \}$$

and where $\sigma_0 = \sigma_o(\mathbf{x})$ is the nominal value of sample material.

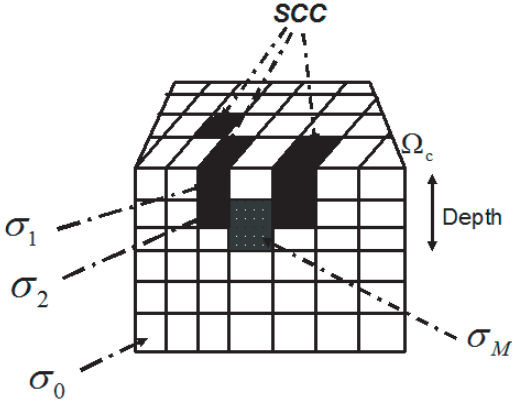


Fig. 2 Crack decompositions.

In order to estimate the recovering internal profiles of SCC by the set of its electrical conductivity corresponding to the set of its sub-region, we construct a parametrized profile SCC function by the set of electrical conductivities $\mathbf{q} = \{\sigma_i\}_{i=1}^M$ defined by

$$\gamma(\mathbf{x}) = \sum_{i=1}^M \sigma_i h_i(\mathbf{x}), \quad (15)$$

where $h_i(\mathbf{x})$ is the characterized function given by

$$h_i(\mathbf{x}) := \begin{cases} 1, & \text{for } \mathbf{x} \in \Omega_{SCC}^k, \quad i = k, \\ 0, & \text{otherwise.} \end{cases} \quad (16)$$

Hence, together with the set of applied alternating currents $\mathbf{J}_s \in (L^2(\Omega))^3$ and the set of the electrical conductivities $(\sigma_0, \{\sigma_k\}_{k=1}^M) \in R^+ \times \mathcal{Q}^M$, then for a fixed angular frequency $\omega \in R^+$, there exists a unique solution $\mathbf{u}(\omega, \mathbf{J}_s) \in \mathcal{V}$

of

$$\alpha_\omega((\sigma_0, \{\sigma_k\}_{k=1}^M); \mathbf{u}, \mathbf{v}) = \beta_{\mathbf{J}_s}(\mathbf{v}), \quad \text{for } \mathbf{v} \in \mathcal{H}. \quad (17)$$

The observation model associated with (13) can be redefined by:

$$\mathcal{Z}^L(\mathbf{q}, \omega, \mathbf{J}_s) = \left\{ \mathcal{Z}_{x_p^l}(\mathbf{q}, \omega, \mathbf{J}_s^l) \right\}_{l=1}^L. \quad (18)$$

Finally, our inverse problem to recover internal profile of SCC is stated as follows. Given the observed data $\mathcal{Z}_d^L = \{\mathcal{Z}_d(\omega, \mathbf{J}_s^l)\}_{l=1}^L$, then find the optimal solution $\mathbf{q} = \mathbf{q}^*$ of

$$\mathcal{F}(\mathbf{q}^*) = \min_{\mathbf{q} \in \mathcal{Q}^M} \frac{1}{2} \sum_{l=1}^L \left| \mathcal{Z}_{x_p^l}(\mathbf{q}, \omega, \mathbf{J}_s^l) - \mathcal{Z}_d(\omega, \mathbf{J}_s^l) \right|^2 \quad (19)$$

subject to the systems (17) and (18).

4. Computational procedure

Our computational procedure is based on the use of finite element Galerkin approach in context of the bilinear form (10). To this end, we consider the set $\{\psi_i^N\}_{i=1}^{4N}$ is the set of finite basis functions in \mathcal{V}^N and \mathbf{u} is the solution of the system (17) related to the systems (1)-(7). Then the approximated solution \mathbf{u}^N of \mathbf{u} can be defined by

$$\mathbf{u}^N = \sum_{i=1}^{4N} \zeta_i^N \psi_i^N,$$

with the coefficient $\zeta^N = \{\zeta_i^N\}_{i=1}^{4N}$ is chosen such that the systems (1)-(7) can be approximated by solving the system

$$F^N(\mathbf{q}) \zeta^N = f^N, \quad (20)$$

where

$$[F^N(\mathbf{q})]_{ij} := \alpha_\omega(\mathbf{q})(\psi_i^N, \psi_j^N)$$

and

$$[f^N]_j := \beta_{\mathbf{J}_s}(\psi_j^N), \quad (21)$$

$i, j = 1, 2, 3, \dots, 4N$.

The corresponding approximate observation (18) can be computed as

$$\mathcal{Z}_L^N(\mathbf{q}, \omega) = \left\{ \mathcal{M}_l \zeta^N(\mathbf{q}, \omega, \mathbf{J}_s^l) \right\}_{l=1}^L, \quad (22)$$

with $[\mathcal{M}_l]_{i,j} = [\mathcal{M}_l]_i \psi_j^N$, $i = 1, 2, j = 1, \dots, 4N$, and

$$\begin{aligned} & [[\mathcal{M}_l]_1 \psi_j^N, [\mathcal{M}_l]_2 \psi_j^N] := \\ & \left[N\omega \oint_{C(x_p^l)} \psi_j^{(N)I} dl_k, \quad -N\omega \oint_{C(x_p^l)} \psi_j^{(N)R} dl_k \right], \end{aligned}$$

$k = 1, 2, 3$, and $l = 1, 2, 3, \dots, L$ and $\psi_j^N = (\psi_j^{(N)R}, \psi_j^{(N)I})$.

Finally, our computational algorithm is to find the parameter vector $\mathbf{q} = \mathbf{q}^*$ which minimizes the error function

$$\mathcal{F}(\mathbf{q}) = \frac{1}{2} \sum_{l=1}^L \left| \mathcal{M}_l \zeta^N(\mathbf{q}, \omega, \mathbf{J}_s^l) - \mathcal{Z}_d(\omega, \mathbf{J}_s^l) \right|^2 \quad (23)$$

with respect to parameter $\mathbf{q} \in \mathcal{Q}^M$ and subject to the systems (22) and (20). Thus, to solve the problem (23) which minimizes the output least square error between the forward problem (22) and (20) and the given simulated data $\{\mathcal{Z}_d(\omega, \mathbf{J}_s^l)\}_{l=1}^L$, we apply a numerical scheme of trust region algorithm with the linearity constraints, a FORTRAN software package "OPT2" (Carter⁽⁶⁾).

5. Numerical experiments

In this section, we present the series of numerical experiments based on the methodology described in the previous section. In the experiments, the dimensions of the conducting material Ω_c were taken as $d_1 \times d_2 \times d_3$ (Fig. 3)

$$d_1 = 17.0, \quad d_2 = 17.0, \quad d_3 = 8.0 \quad [\text{mm}].$$

In order to solve the system (20), then the system model Ω_c in Fig.3 was discretized by a finite element method with the number of finite elements and nodes were set as $17 \times 17 \times 8 = 2312$ elements and 2961 nodes, respectively.

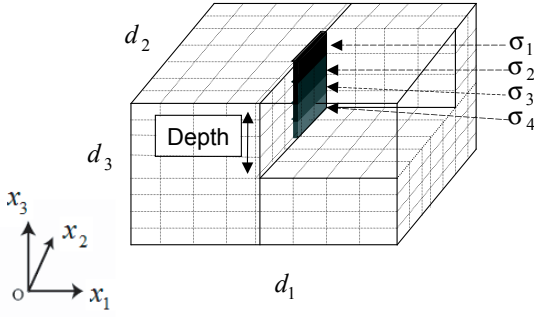
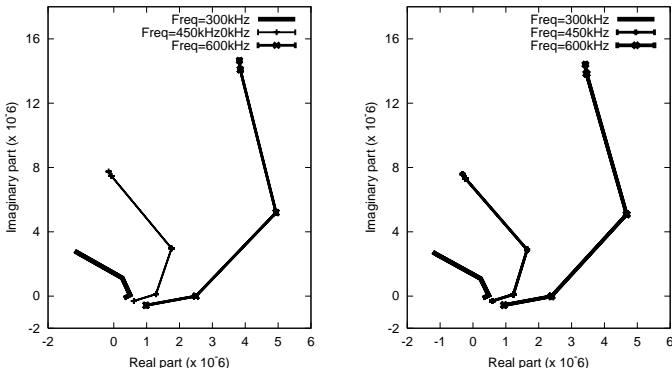


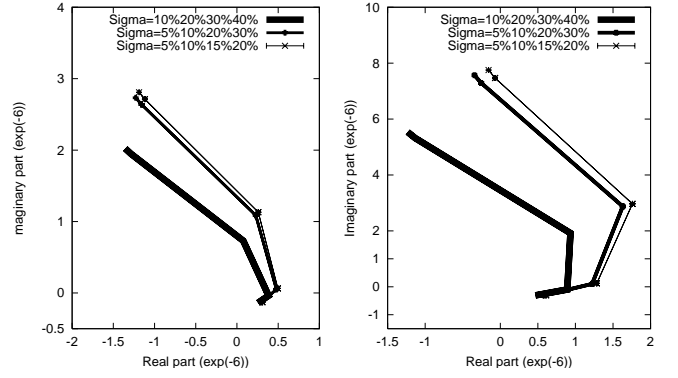
Fig. 3 Characterization of crack parameters.



(a) Simulation results with $\mathbf{q} = \{5\% \times \sigma_0, 10\% \times \sigma_0, 15\% \times \sigma_0, 20\% \times \sigma_0\}$.

(a) Simulation results with $\mathbf{q} = \{5\% \times \sigma_0, 10\% \times \sigma_0, 20\% \times \sigma_0, 25\% \times \sigma_0\}$.

Fig. 4 Simulation results of ECT signal with various frequencies for forward problem.



(a) Simulation results with frequency $f = 300[\text{kHz}]$.

(a) Simulation results with frequency $f = 450[\text{kHz}]$.

Fig. 5 Simulation results of ECT signal with the frequencies 300[kHz] in (a) and 450[kHz] in (b) for forward problem.

The physical parameters are given by

$$\sigma_0 = 1.39 \times 10^6 [\text{Sm}^{-1}] \quad \text{and} \quad \mu_0 = 4\pi \times 10^{-7} [\text{Hm}^{-1}]$$

and the set of alternating currents and the number of observation points were taken as

$$\mathbf{J}_s^l = 1.0[\text{A}], \quad \text{for } l = 1, \dots, L, \\ L = 9.$$

Moreover, in our test examples, we use the crack modeling as depicted in Fig.3, with the crack depth = 4[mm], length = 9[mm] and width = 1[mm], located in the center of the conducting material Ω_c . By decomposing the crack modeling into $M=4$ sub-crack regions, then the crack parameter in (15) can be preassigned as $M = 4$. Therefore, the parametrized internal profile of SCC is then defined by

$$\gamma(\mathbf{x}) = \sum_{i=1}^4 \sigma_i h_i(\mathbf{x}), \quad (24)$$

with the lower and upper bounds for $\mathbf{q} = \{\sigma_i\}_{i=1}^4$ are

$$1\% \times \sigma_0 \leq \sigma_i \leq 90\% \times \sigma_0, \quad i = 1, 2, 3, 4.$$

Numerical experiments for the forward problems can be obtained by solving the systems (20) and (22). In these experiments, frequency is a very important factor since the depth of penetration of eddy current \mathbf{J}_e will depend on the skin depth δ calculated by

$$\delta = \frac{1}{\sqrt{\pi \sigma_c \mu_0 f}}. \quad (25)$$

Fig.4 depicts the sensitivity of algorithm with respect to the various frequencies conducted in the simulation, while Fig.5 depicts the sensitivity of algorithm with respect to the chosen various set of electrical conductivities $\{\sigma_i\}$ corresponding to its sub-region Ω_{SCC}^i .

Table 1 Estimated value using frequency $f = 300.00$ [kHz].

True value = $\{\sigma_1, \sigma_2, \sigma_3, \sigma_4\} = \{5.0\%, 10.0\%, 15.0\%, 20.0\% \}$ ($\times \sigma_0$)				
Estimated value with Noise free , Iteration = 9				
	σ_1	σ_2	σ_3	σ_4
$\sigma_i (\times \sigma_0)$	5.4379%	8.7102%	11.5966%	15.4228%
Relative error (%)	8.7580	12.8980	22.6893	22.8860
5% Noise, Iteration = 9				
$\sigma_i (\times \sigma_0)$	5.6523%	8.5718%	11.4629%	15.2239%
Relative error (%)	13.0460	14.2820	23.5807	23.8805
10% Noise , Iteration =9				
$\sigma_i (\times \sigma_0)$	4.6333%	8.3878%	11.2513 %	15.3680 %
Relative error (%)	7.3340	16.1220	24.9913	23.1600
15% Noise , Iteration = 9				
$\sigma_i (\times \sigma_0)$	4.2988%	7.6970%	10.6797%	15.1726%
Relative error (%)	14.0240	23.0300	28.8020	24.1370

Table 2 Estimated value using frequency $f = 450.00$ [kHz].

True value = $\{\sigma_1, \sigma_2, \sigma_3, \sigma_4\} = \{5.0\%, 10.0\%, 15.0\%, 20.0\% \}$ ($\times \sigma_0$)				
Estimated value with Noise free , Iteration = 8				
	σ_1	σ_2	σ_3	σ_4
$\sigma_i (\times \sigma_0)$	5.5336%	8.9429%	11.4153%	15.2068%
Relative error (%)	8.672	10.5710	23.8980	23.9660
5% Noise, Iteration = 8				
$\sigma_i (\times \sigma_0)$	5.7894%	8.4939%	11.5267%	15.4135%
Relative error (%)	15.7880	15.0610	23.1553	22.9325
10% Noise , Iteration =8				
$\sigma_i (\times \sigma_0)$	4.5998%	9.0127%	12.3464 %	15.7283%
Relative error (%)	8.0040	9.8730	17.6907	21.3585
15% Noise , Iteration = 8				
$\sigma_i (\times \sigma_0)$	4.3913%	7.9831%	11.8344%	15.5147%
Relative error (%)	12.1740	20.1690	21.1104	22.4265

Table 3 Estimated value using frequency $f = 600.00$ [kHz].

True value = $\{\sigma_1, \sigma_2, \sigma_3, \sigma_4\} = \{5.0\%, 10.0\%, 15.0\%, 20.0\% \}$ ($\times \sigma_0$)				
Estimated value with Noise free , Iteration = 8				
	σ_1	σ_2	σ_3	σ_4
$\sigma_i (\times \sigma_0)$	4.7562%	9.6365%	12.3307%	15.5789%
Relative error (%)	4.8760	3.6310	17.7953	22.1055
5% Noise, Iteration = 9				
$\sigma_i (\times \sigma_0)$	4.3929%	10.3269%	12.3664%	15.4486%
Relative error (%)	12.1420	3.2690	17.5573	22.7570
10% Noise , Iteration =9				
$\sigma_i (\times \sigma_0)$	4.3157 %	9.0552 %	11.7929 %	15.3774%
Relative error (%)	13.6860	9.4480	21.3807	23.1130
15% Noise , Iteration = 9				
$\sigma_i (\times \sigma_0)$	4.2279%	8.0355%	11.3282%	15.2685%
Relative error (%)	15.4420	19.6450	24.4787	23.6575

For the inverse problems, carrying out a number of numerical simulations, we summarize in Tables 1-5 our computational simulations related to characterize internal profiles of SCC parameters $\mathbf{q} = \{\sigma_1, \sigma_2, \sigma_3, \sigma_4\}$ using the proposed method given by the set of the simulated data $\{\mathcal{Z}_d(\omega, \mathbf{J}_s^l)\}_{l=1}^L$ generated by solving the systems (20) and (22). Random noise at various level was added to the numerical solution, thereby producing simulated noise data for algorithm.

In Tables 1-5, the initial guesses were taken as

$$\{\sigma_1, \sigma_2, \sigma_3, \sigma_4\} = \{1\% \times \sigma_0, 1\% \times \sigma_0, 1\% \times \sigma_0, 1\% \times \sigma_0\}$$

while the true parameters in Tables 1-3 were chosen as

$$\{\sigma_1, \sigma_2, \sigma_3, \sigma_4\} = \{5\% \times \sigma_0, 10\% \times \sigma_0, 15\% \times \sigma_0, 20\% \times \sigma_0\}$$

and in Tables 4-5 were

$$\{\sigma_1, \sigma_2, \sigma_3, \sigma_4\} = \{5\% \times \sigma_0, 10\% \times \sigma_0, 20\% \times \sigma_0, 25\% \times \sigma_0\}.$$

The applied frequencies f were given as 300[kHz] in Tables 1 and 4, $f = 450$ [kHz] in Tables 2 and 5 and $f = 600$ [kHz] in Table 3. The estimated parameter values listed in Tables 1-5 are for the data with noise free and with data containing 5, 10 and 15% relative noise. The relative error was computed as

$$Relative\ error = \left| \frac{Estimated\ value - True\ value}{True\ value} \right| \times 100\%.$$

Table 4 Estimated value using frequency $f = 300.00$ [kHz].

True value = $\{\sigma_1, \sigma_2, \sigma_3, \sigma_4\} = \{5.0\%, 10.0\%, 20.0\%, 25.0\%\}$ ($\times \sigma_0$)				
Estimated value with Noise free , Iteration = 9				
	σ_1	σ_2	σ_3	σ_4
$\sigma_i (\times \sigma_0)$	5.6858%	7.9746%	15.8983%	20.1957%
Relative error (%)	13.7160	20.2540	20.5085	19.2172
5% Noise, Iteration = 9				
$\sigma_i (\times \sigma_0)$	5.5586%	7.8163%	15.7840%	20.1688%
Relative error (%)	11.1720	21.8370	21.0800	19.3248
10% Noise , Iteration =9				
$\sigma_i (\times \sigma_0)$	4.5195 %	7.3401 %	15.7009 %	20.1589 %
Relative error (%)	9.6100	26.5990	21.4955	19.3764
15% Noise , Iteration = 9				
$\sigma_i (\times \sigma_0)$	4.5687%	7.5813%	18.3691%	20.9859%
Relative error (%)	8.6260	24.1870	8.1545	16.0564

Table 5 Estimated value using frequency $f = 450.00$ [kHz].

True value = $\{\sigma_1, \sigma_2, \sigma_3, \sigma_4\} = \{5.0\%, 10.0\%, 20.0\%, 25.0\%\}$ ($\times \sigma_0$)				
Estimated value with Noise free , Iteration = 8				
	σ_1	σ_2	σ_3	σ_4
$\sigma_i (\times \sigma_0)$	5.4632%	8.6749%	16.3504%	20.3102%
Relative error (%)	9.2640	13.2510	18.2480	18.7592
5% Noise, Iteration = 8				
$\sigma_i (\times \sigma_0)$	4.7162%	11.8700%	19.7559%	21.4432%
Relative error (%)	5.6760	18.7000	1.2205	14.2272
10% Noise , Iteration =8				
$\sigma_i (\times \sigma_0)$	4.7679%	8.5747%	16.6777%	20.4537%
Relative error (%)	4.6420	14.2530	16.6115	18.1852
15% Noise , Iteration = 8				
$\sigma_i (\times \sigma_0)$	4.8959%	8.5660%	16.5688%	20.1251%
Relative error (%)	2.0820	14.3400	17.1560	19.4996

As shown in Tables 1-3, the relative errors in the estimated value results of each row tend to be bigger as the index i increases, since those are caused by the depth δ given by (25). Hence the resolution of our inverse problem depends on the physical environments inspected.

6. Concluding remarks

A computational method was considered to recover internal profiles of stress corrosion cracking related to eddy current testing. The method for recovering is directed to electromagnetic inverse problem by characterizing each sub-region of the SCC decomposition using its non-zero electrical conductivity, while an estimation technique for inverse analysis is proposed by a hybrid use of the forward analysis and inspection data. This method is an important feature for the problem of recovering internal profiles treated here. The proposed inverse analyses for recovering internal profile of SCC were successfully tested with the simulated data.

Our current study is directed to the inverse problem for the more complicated structures of SCC and the computational problem with experimental data.

References

- (1) A. Ausri and F. Kojima: Computational methods for estimating deep-lying profiles of stress corrosion cracking arising in eddy current testing, Transactions of the JASCOME Journal of Boundary Element Methods **7**-1 (2007), pp. 85-90.
- (2) F. Kojima and A. Ausri: Identification of stress corrosion cracking of SUS samples arising in electromagnetic nondestructive testing, J.Inv. Ill-Posed Problems, **15**-8 (2007), pp. 799-812.
- (3) F. Kojima: Defect shape recovering by parameter estimation arising in eddy current testing, Journal of the Korean Society for Nondestructive Testing **23**-6(2003), pp. 622-634.
- (4) F. Kojima: Inverse problems related to electromagnetic nondestructive evaluation, Research Directions in Distributed Parameter Systems (R.C. Smith and M.A. Demetriou Eds.), SIAM Frontiers in Applied Mathematics **FR-27**(2003), pp. 219-236.
- (5) S.J. Norton and J.R. Bowler: Theory of eddy current inversion, Journal of Applied Physics **73**-2(1993), pp. 501-511.
- (6) R.G. Carter: On the global convergence of trust region algorithms using inexact gradient information, Technical Report 87-6, Rice University, (1987).